

## The Role Of Ply Orientation On The Resin Flow Under Compaction In Thermoplastic Composites

Jimenez del Toro, Alejandro; Teuwen, Julie J.E.

**Publication date**

2024

**Document Version**

Final published version

**Published in**

Proceedings of the 21st European Conference on Composite Materials

**Citation (APA)**

Jimenez del Toro, A., & Teuwen, J. J. E. (2024). The Role Of Ply Orientation On The Resin Flow Under Compaction In Thermoplastic Composites. In C. Binetury, & F. Jacquemin (Eds.), *Proceedings of the 21st European Conference on Composite Materials: Volume 5 - Manufacturing* (Vol. 5, pp. 540-547). The European Society for Composite Materials (ESCM) and the Ecole Centrale de Nantes..

**Important note**

To cite this publication, please use the final published version (if applicable).  
Please check the document version above.

**Copyright**

Other than for strictly personal use, it is not permitted to download, forward or distribute the text or part of it, without the consent of the author(s) and/or copyright holder(s), unless the work is under an open content license such as Creative Commons.

**Takedown policy**

Please contact us and provide details if you believe this document breaches copyrights.  
We will remove access to the work immediately and investigate your claim.

## THE ROLE OF PLY ORIENTATION ON THE RESIN FLOW UNDER COMPACTION IN THERMOPLASTIC COMPOSITES

Alejandro Jimenez del Toro<sup>1</sup>, Julie J. E. Teuwen<sup>2</sup>

<sup>1,2</sup>Department of Aerospace Structures and Materials, Delft University of Technology, Kluyverweg 1, Delft, 2629 HS, The Netherlands

<sup>1</sup>Email: a.jimenezdeltoro@tudelft.nl

<sup>2</sup>Email: j.j.e.teuwen@tudelft.nl

**Keywords:** thermoplastics, compaction, percolation flow, squeeze flow, ply orientation

### Abstract

In this study, a gap filling methodology was used to evaluate the flow behaviour of carbon fibre reinforced polyphenylene sulphide (CF/PPS) tapes under various compaction conditions (force and time) and layups. At each side of the gap, a different layup was present: 0/0 and 0/90. It was observed that squeeze flow occurred under all compaction forces and times, increasing with them. The layup influenced the squeeze flow development significantly, particularly visible in the change of the 0° fibre angle of the substrate across the gap. This fibre angle increased from the 0/90 to the 0/0, as the latter showed more squeeze flow than the former due to the parallel layup. The change of fibre angle across the substrate's width was indicative of the extent of the squeeze flow along its width. The percolation flow increased with compaction force and time, and both longitudinal and transverse flow were found. Longitudinal flow was visible at larger compaction forces, whereas transverse flow was the only flow found at lower ones. The development of transverse over longitudinal percolation flow is influenced by the layup, the sample configuration and the squeeze flow.

### 1. Introduction

Rapid processability of carbon fibre reinforced thermoplastic composites relies on effectively consolidating the laminates in a limited period of time. Such consolidation requires the development of intimate contact between the plies, plus the healing of the interfaces. Intimate contact development involves the flow of the composite under pressure, which would bring the thermoplastic matrix at both sides of the interface into contact.

Two types of flow are present in continuous fibre thermoplastic composites under compaction, squeeze and percolation flow. These flows can remove the surface asperities present in tapes and flatten the interfaces between two tapes for intimate contact. Squeeze flow involves the flow of fibres and matrix together in the transverse direction, widening the composite tape. Squeeze flow is highly anisotropic due to the presence of inextensible fibres in the longitudinal direction, which prevent deformation. Percolation is the flow of resin in the longitudinal and transverse direction to the fibre bed. The fibre bed permeability plays a significant role in the development of this flow. Such permeability is limited in both longitudinal and transverse directions, being one order of magnitude lower in the later [1]. The compact packing of the fibres and their small diameter contribute to the increased tortuosity in this direction. Simultaneously, the fibres impose a large extensional viscosity on the molten thermoplastic along their length.

Intimate contact models, to predict extent of flow in TP tapes during processing, based solely on the squeeze flow under compaction have been proposed and widely used. Yet, Celik et al. [2] showed that squeeze flow based intimate contact models could not successfully predict the experimental degree of intimate contact in CF reinforced polyetheretherketone single tape experiments in AFP. The authors concluded that squeeze flow and percolation flow, in both longitudinal and transverse directions, were

present, filling matrix poor areas at the surface of the tape. Thus, studying the contribution of each flow mode to the total flow of composites under different compaction conditions can lead towards further understanding the development of intimate contact.

In addition to the influence of the fibre orientation on the flow development within a tape, the orientation of the substrate on which it is placed can play a significant role too. It has been shown that substrate orientation can alter the squeeze flow behaviour in cross-ply layups [3]. The presence of inextensible fibres in different directions hinders the squeeze flow development of the whole layup. In doing so, percolation could then be promoted and found to be a greater contributor to the overall composite deformation [4]. Given the layup design flexibility in AFP, analysing the effect of the relative orientation between tape and substrate on the flow development is of relevance.

Mostly indirect methods of evaluating the different flow modes have been considered in literature so far. Kermani et al. [5] and Simacek et al. [6] developed a methodology to study the contribution of squeeze and transverse percolation flow in the gap filling process of composites. Their sample was a  $0^\circ/90^\circ/0^\circ$  cross-ply laminate made of unidirectional, continuous carbon fibre reinforced thermoset prepreg. The middle layer consisted of  $90^\circ$  plies with predefined gaps between them. The samples were compacted in an autoclave and the gap filling process was characterised by cross-sectional optical microscopy. The squeezed and percolated regions were visible, quantified. Their experimental results showed that percolation was the main contributor to the gap filling process and predicted a positive correlation between the increase in fibre bed permeability and the reduction of sample's thickness to the increase in transverse percolation flow.

The aim of this paper is to study the different flow modes during consolidation of thermoplastic composites for different ply orientations and compaction settings. Therefore, the setup described in [5,6] was adapted to, on top of squeeze flow and transverse percolation, also capture percolation in the longitudinal direction and the effect of ply orientation. We studied the behaviour of carbon fibre polyphenylene sulphide (CF/PSS) tapes in (0/0) and (0/90) orientation in a gap filling process performed in a dynamic-mechanical analyser (DMA) at different compaction forces and times. Optical microscopy was used to analyse the flow modes and to measure the resulting fibre angles due to squeeze flow.

## 2. Materials and Methods

The material used in this study is CF/PSS unidirectional tapes (Suprem®) with a fibre volume fraction of 55%. The tape's thickness and width are 0.15 mm and 6.35 mm, respectively. The nominal melting point of the resin is 280 °C, as measured by differential scanning calorimetry.

The specimen comprises two layers made with three tapes in total. Each tape is 6.35 mm wide, 0.15 mm thick and approximately 2 cm long. The substrate consists of one unidirectional tape oriented at  $0^\circ$ . The second layer consists of two tapes separated by a gap of 0.6 mm width and 6.35 mm length. One of the tapes is placed at a  $0^\circ$  orientation and the other at  $90^\circ$ . A small gap width was chosen to prevent or minimise protrusion of the substrate into the gap. Local compaction on the gap area is applied by an aluminium metal plate of 10 mm in width and 14 mm in length. This also allows to reach larger compaction pressures on the sample, as the DMA used is limited to 30 N of force. This generates a compaction width of 4.5 mm on each tape, and a total compaction area of roughly 60 mm<sup>2</sup>. A representation of the sample layout and compaction area can be found in Figure 1a. Two fibre orientations are facing the gap, so that all three flow modes can contribute towards the gap filling process: squeeze flow and percolation flow in the transverse direction from the  $90^\circ$  tape (side A in Figure 1b), and longitudinal percolation from the  $0^\circ$  tape (side B in Figure 1b). In addition, the effect of the relative orientation between substrate and tape on the transverse squeeze and percolation behaviour can be assessed from the comparative analysis of sides A and C, as seen in Figure 1b, where side A represents a 0/90 layup and side C a 0/0 layup.

The samples are processed in a RSA G2 DMA (TA Instruments) with a 25 mm in diameter compression fixture. Between the metal plates and the composite, Kapton® tape is used to prevent them to stick. The

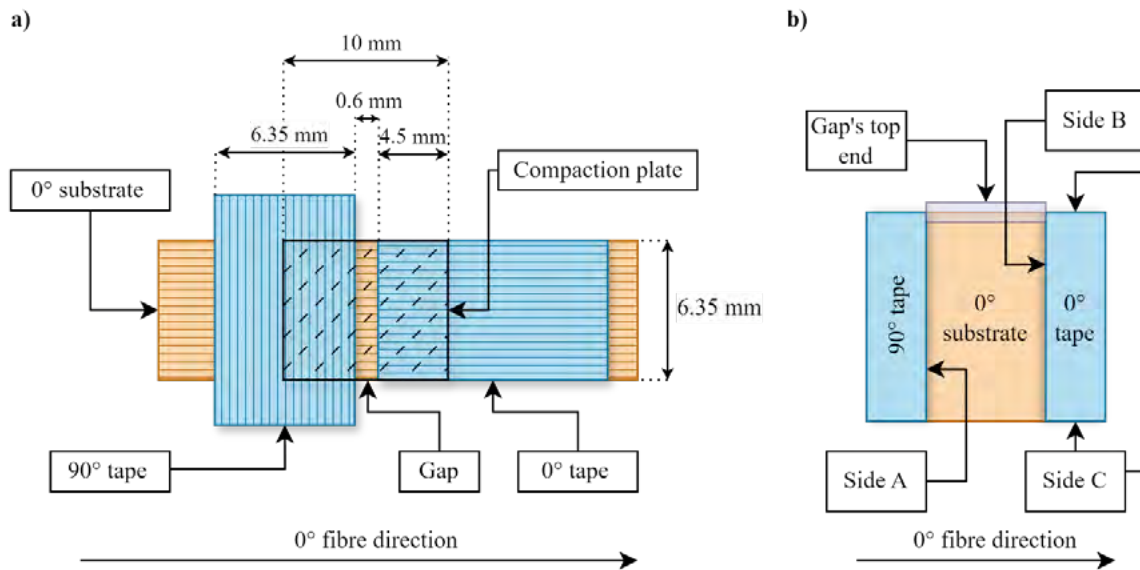


**Figure 1.** a) Schematics of the sample layout and the compaction area. The 3 CF/PPS ply arrangement including the gap between the two top tapes is shown. The compaction area is represented as a dashed area. b) Close up schematics of the gap area with the indication of the sides of interest (A, B, C, gap's top end) for the experiments

selected compaction forces,  $F_c$ , are 12 N and 24 N, which result in approximately 200 and 400 kPa of pressure, respectively. These forces are representative for AFP-like processing conditions. The tested compaction times,  $t_c$ , are 250 and 500 s. A force of 0.05 N and compaction time of 500s were used as a baseline. The different sample identifiers and their processing conditions can be found in Table 1. The samples are produced using an isothermal compaction program, so that the contribution of the temperature to the viscosity of the matrix is kept constant. At first, the temperature is increased from 40 to 360 °C at 10 °C/min, with a holding pressure of 0.05 N. The ramp is followed by an isothermal step at 360 °C, where the targeted compaction force,  $F_c$ , and time,  $t_c$ , are applied. At the end of this step, the sample is cooled down to 25 °C at 10 °C/min and a holding pressure of 0.05N is applied. The DMA program is represented in Figure 2.

The characterisation of the different flows in the sample is done by means of optical microscopy using a VK-X1000 confocal scanning microscope (Keyence®). The squeeze flow deformation of sides A and C is defined as the tape's maximum width increase with respect to the original tape's width. The original tape width is defined as the width of the tape that is not under the compaction plate. Note that, as there are two sides C, the final side C deformation reported is the average of both sides, so that it can be compared to side A. The effect of different layups on squeeze flow behaviour of the substrate is characterized by analysing the change of the substrate's fibre angle across the gap's width, as fibres transition from a 0/90 layup on side A to a 0/0 layup on side B. The resulting fibre angles observed in the substrate are calculated with respect to the original 0° fibre angle of the substrate and are evaluated along the gap's length, from the its top end, i.e. 0 µm, see Figure 1b, to approximately the middle line of the gap, i.e. 3000 µm. The other half of the gap is considered symmetrical. Only the visible fibres could be measured. As a significant degree of scatter in the fibre angle was found, the gap's length was divided in 200 µm sections. For each section, the average fibre angle and its standard deviation were estimated, when more than one fibre was identified. Finally, the extent of percolation flow was estimated by the ratio of the resin-covered gap length to the total gap length in the tested samples.

**Table 1.** Process conditions used in DMA for compaction force and time with their corresponding sample identification labels.

Sample ID	Compaction force, N	Compaction time, s
Reference	0.05	500
12A	12	250
12B		500
24A	24	250
24B		500

### 3. Results

The gap micrographs for all tested samples can be found in Figure 3. Firstly, the gap filling in terms of percolated resin will be presented. The isothermal compaction of the samples results in resin percolation within the gap when a force of 24 N is applied (Figure 3d and 3e). At longer compaction times (24B), the resin fills 83% of the gap's length while for shorter times (24A) it is 42%. The matrix front across the gap width is higher at side B (0/0) compared to side A (0/90) for longer compaction times (24B), while this is not visible in 24A, as both sides are equally covered. In addition, a matrix droplet can be seen on side A (0/90) for shorter compaction times (24A). Samples at lower compaction forces (12A and 12B) do not show gap filling, Figure 4b and 4c; yet, for longer compaction times (12B), droplets of matrix are spotted at side A (0/90). The reference sample, Figure 4a, does not display any percolated resin within the gap area. No percolated resin was found on side C (0/0) for any test configuration.

Secondly, squeeze flow is also observed after the experiments, on side C (squeeze flow of the 0/0 layer) and side A (squeeze flow of the 90 layer), see Figure 4 for maximum width increase observed at these locations. Squeeze flow is observed on side C at all forces and compaction times. The same holds for side A except for the reference case of 0.05 N force. The largest squeeze flow of side C is measured for the highest compaction force and time (24B) and it decreases with both. The effect of the compaction force is far more noticeable than that of time. A similar behaviour is found for side A (0/90), yet the percolated resin does not allow to accurately determine the squeezed front for the highest force (24A and 24B), thus no further analysis can be conducted on this.

Also a change in the original 0° fibre angle of the substrate is observed across the gap's width, as it is clearly visible in Figure 3e and 3d compared to 3a. Figure 5 shows the averaged fibre angle along approx. half of the gap's length as a function of the compaction conditions. The fibre angles reach a maximum value,  $\theta_{max}$ , close to the free edge and increase with both force and time under compaction. We observed a range of  $\theta_{max}$  from 4.5%-15.9% for the different compaction setting, see also Figure 4. After that, all samples, except for the reference, show an asymptotic decreasing trend towards the middle of the tape width, where the values converge to the angles of the reference sample (indicative values of their initial fibre angle of 0°). Note that the percolated resin in sample 24B does not allow to characterise the fibre angle beyond 800  $\mu\text{m}$ . The distance over which the fibre angles decrease towards 0° also increases with the compaction force and time.

## 4. Discussion

### 4.1. Squeeze flow

The squeeze flow measured on side C of the tape increases with both force and time, as expected. The effect of the compaction force is more significant than that of the compaction time. A 3% increase in tape's width is seen between 250 and 500 s for both compaction forces, 12 and 24 N. Doubling the compaction force, from 12 to 24 N, induces a 5% increase on the tape's width for both compaction

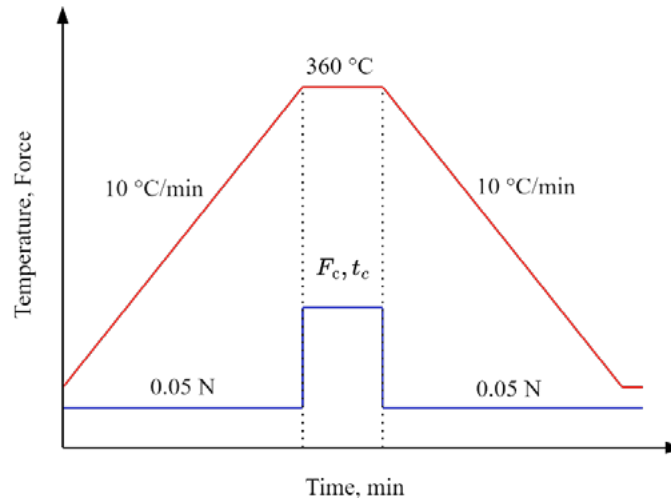


**Figure 2.** DMA temperature and force profile schematics. The values of the compaction force,  $F_c$ , and time,  $t_c$ , can be found in Table 1.

times. This can be related to the larger deformation rate achieved by applying larger compaction forces. The squeeze flow observed on side A is 1% lower than that of side C for the reference and 12A samples, while they are equal for 12B. The layup does not seem to play a significant role on the maximum width increase between sides A and C for the samples tested at 12 N.

On the substrate, the increase of fibre angle across the gap's width can be related to a more developed squeeze flow of the 0/0 layup compared to the 0/90 one. The perpendicular, inextensible fibres of the 0/90 layup constrain the squeeze flow of the substrate, maintaining the original  $0^\circ$  angle of the substrate's fibres, as observed in Figure 3d and 3e. On the contrary, the substrate is able to further develop squeeze flow on a 0/0 layup, due to the cooperative movement between two plies with parallel fibres. The displacement of fibres, along with the resin, in the transverse direction of the substrate generates a distortion of the fibre angle across the gap. As seen in Figure 4, the measured  $\theta_{max}$  increases with compaction force and time, as it would be expected for squeeze flow, and correlates well with the deformation of side C. The observed differences on the effect of the layup on the squeeze flow behaviour of the substrate and the tapes are not yet clear from these experiments.

The change in fibre angle with the distance to the gap end can be interpreted as the squeeze flow developing across the substrate's width. Figure 5 shows that the extent of the squeeze flow across the gap length is a function of both, the compaction force and time, with larger times and forces inducing larger affected areas. The fibres near to the edge of the gap are the most affected ones, registering a larger angle change. The closer to the middle line of the substrate, at approximately  $3000 \mu\text{m}$ , the lesser the angle of the fibres, indicating a less developed squeeze flow across the substrate's width. As the squeeze flow induces a change in the fibre bed arrangement and therefore its permeability, this could affect the development of percolation flow across the substrate's width. Hence, the different flow modes could have a heterogeneous contribution to the intimate contact development across the width of the compacted tape.

#### 4.2. Percolation flow

Percolation flow is found to contribute more towards the gap filling process with increasing compaction forces and times. Due to the limited tested compaction forces and times, there are not enough data points to track the evolution of the percolated matrix for all samples. Yet, two distinct percolation modes are found as a function of the compaction force after 500 s.

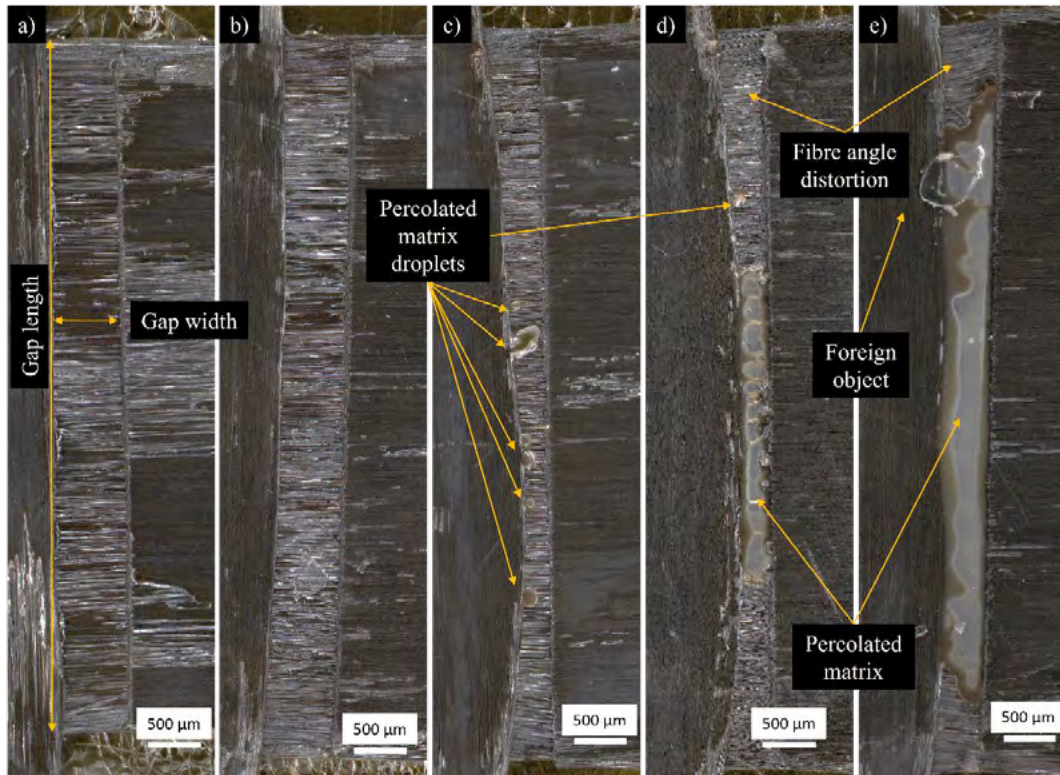


**Figure 3.** Gap micrographs for all tested samples (top view, showing sides A and B from Figure 2), for different compaction settings (see Table 1), as a) Reference, b) 12A, c) 12B, d) 24A and e) 24B. The magnification used for all micrographs is 12x. Features highlighted in the figures are gap length and width, in a); percolated matrix droplets, in c) and d); fibre angle distortion and percolated matrix in d) and e); foreign object in e).

A higher compaction force (24B) has a larger percolation contribution to the gap filling compared to a lower one (12B), which indicates a strong dependency of the percolation flow with the compaction force (Figure 4c and 4e). The greater coverage of resin on side B (0/0) compared to side A (0/90) in the gap area suggests that the resin front across the gap originated from side B, indicating that longitudinal percolation is present in 24B. The individual contribution of longitudinal and transverse percolation flow to the gap filling process of sample is not measurable from this characterisation. The lack of longitudinal percolation flow at a lower compaction force (12B) suggests a compaction force dependence on the preferred percolation mode.

At a lower compaction force (12B), the sample has matrix droplets throughout its side A (0/90), as seen in Figure 4c. These can be related to transverse percolation occurring upon these conditions. Yet, no longitudinal percolation is found on side B (0/0), which has a higher permeability and therefore should be preferred. Furthermore, no transverse percolation is found in side C either (0/0), which undergoes the same deformation upon compaction as side A. The lack of percolation flow on sides B and C can be attributed to the development of squeeze flow in both the substrate and the tape in the 0/0 layup. This would ease the localised pressure on both sides as it allows the widening and thinning of the 0/0 stack, hindering the development of any percolation flow. To the contrary, a higher localised pressure would be found on side A (0/90), as the cooperative squeeze flow of tape and substrate is not possible.

In addition, two more factors contribute towards the development of transverse percolation flow. First, both ends of the 90° tape extend beyond the compaction area, effectively blocking the more favourable longitudinal percolation flow. And, second, as side A undergoes squeeze flow upon compaction, the initial fibre bed permeability is altered, which can further contribute towards easing transverse

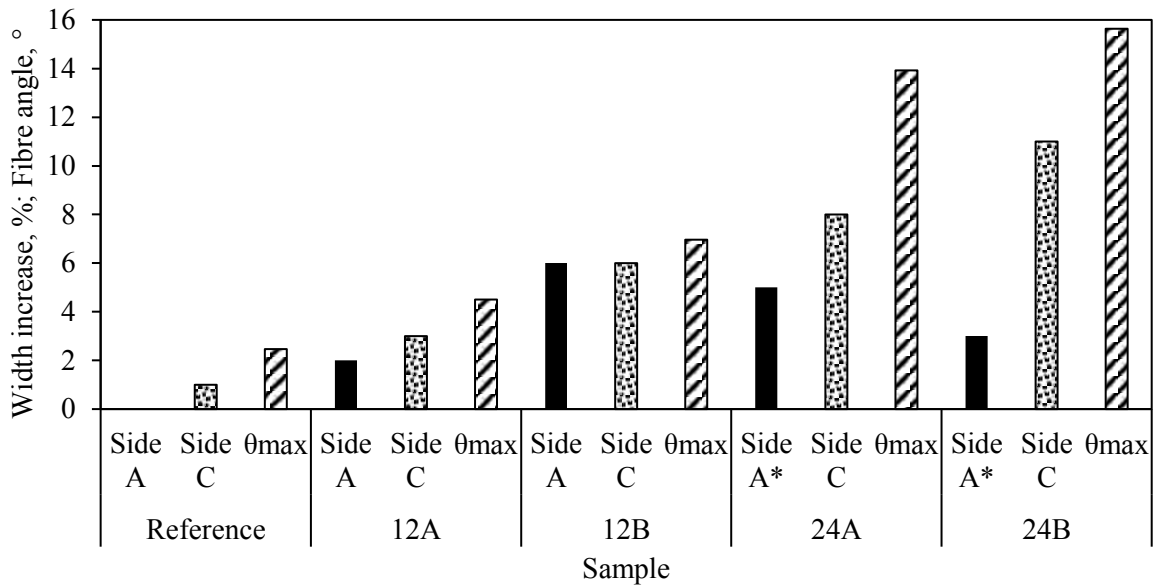


**Figure 4.** Results for the maximum width increase of sides A and C and the maximum fibre angle change within the gap area for all tested configurations. The \* indicates not conclusive values.

percolation. The lesser squeeze flow found at lower compaction times (12A) would be responsible for the lack of transverse percolation in these conditions. Finally, it is also worth noting the lack of transverse percolation on side C at higher compaction forces (24B), which clearly indicates that compaction force and squeeze flow are not enough to promote transverse percolation over the more favourable squeeze and longitudinal percolation flows. Instead, the layup and the boundary conditions of the compacted area have a significant influence on the preferred percolation flow.

## 5. Conclusions

In this work, an experimental gap filling methodology was successfully applied on CF/PPS composites. It allowed to evaluate the different flow modes of the composite upon different compaction conditions and layups. At each side of the gap, a different layup was present: 0/90 and 0/0. Squeeze flow was found at all tested compaction forces and times, and was force and time dependent. The effect of the layup on the squeeze flow development was clearly seen in the change of the original 0° fibre angle of the substrate across the gap area. The 0/90 layup hindered the squeeze flow of the substrate due to the presence of inextensible fibres in the 90° direction, retaining more effectively its original width and therefore the 0° angle of the fibres. The 0/0 layup allowed the cooperative squeeze flow of substrate and tape, widening the substrate. The fibre displacement due to squeeze flow imposed a fibre angle change across the gap, which indicated the extent of the squeeze flow across the width of the substrate. The gradient in fibre angle can also be related to a gradient in the fibre bed permeability, which could impose a heterogenous flow behaviour across the width of the compacted tape.

The percolation flow was also found to increase with compaction force and time, yet the preferred flow mode was influenced by the layup and the boundary conditions around the compacted area. Longitudinal percolation flow was present at higher compaction forces, as the resin front in the gap developed from the 0° tape at the 0/0 layup. Transverse percolation was favoured at lower compaction forces from the 90° at the 0/90 layup, where no longitudinal flow was found. This is due to several factors: first, the increased localised pressure in the 0/90 layup due to the lack of squeeze flow of the substrate; second, the squeeze flow of the 90° tape increases the transverse permeability; and, third, both ends of the 90° extended outside the compacted area, blocking the longitudinal flow. Thus, the preferred percolation flow is a function not only of the compaction force and time, but also the layup



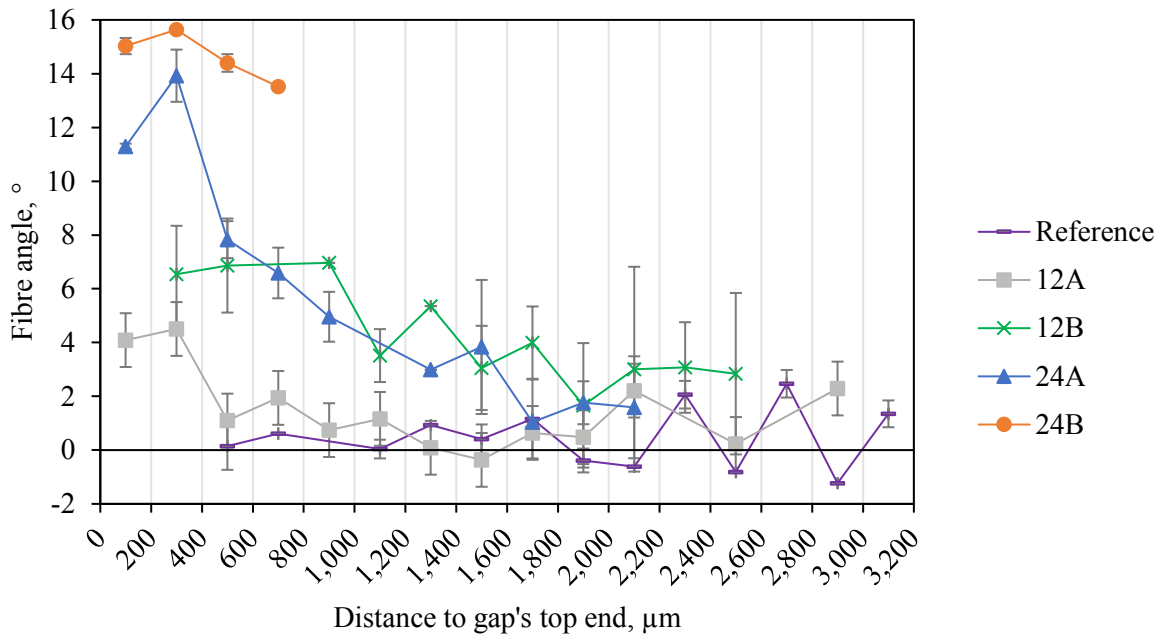


**Figure 5.** Evolution of averaged fibre angle along the gap's length at 200  $\mu\text{m}$  intervals for each tested configuration.

and boundary conditions of the compacted area. These findings can help understand how the composite flow develops in AFP and convey strategies to improve intimate contact development.

Future work will include: (1) expanding these experiments to more compaction forces, times and layups in DMA as well as in AFP; (2) isolating each flow mode by having the same layup at both sides of the gap; and (3) using cross-sectional microscopy and micro-CT to determine the contribution of each flow mode to the gap filling process, as well as the role of fibre bed permeability on the transverse and longitudinal percolation.

## References

- [1] Amin, M, et al. "Longitudinal and Transverse Flows in Fiber Tows: Evaluation of Theoretical Permeability Models through Numerical Predictions and Experimental Measurements." *Composites Part A: Applied Science and Manufacturing*, vol. 119, 1 Apr. 2019, pp. 73–87, <https://doi.org/10.1016/j.compositesa.2018.12.032>.
- [2] Çelik, Ozan, et al. "Intimate Contact Development during Laser Assisted Fiber Placement: Microstructure and Effect of Process Parameters." *Composites Part A: Applied Science and Manufacturing*, vol. 134, July 2020, p. 105888, <https://doi.org/10.1016/j.compositesa.2020.105888>.
- [3] Kobler, Eva, et al. "Modeling the Anisotropic Squeeze Flow during Hot Press Consolidation of Thermoplastic Unidirectional Fiber-Reinforced Tapes." *Journal of Thermoplastic Composite Materials*, 20 Nov. 2023, <https://doi.org/10.1177/08927057231214458>.
- [4] J.A. Goshawk, et al. "Squeezing Flow of Continuous Fibre-Reinforced Composites." *Journal of Non-Newtonian Fluid Mechanics*, vol. 73, no. 3, 1 Dec. 1997, pp. 327–342, [https://doi.org/10.1016/s0377-0257\(97\)00049-9](https://doi.org/10.1016/s0377-0257(97)00049-9).
- [5] Niknafs Kermani, Navid, et al. "Gap Filling Mechanisms during the Thin Ply Automated Tape Placement Process." *Composites Part A: Applied Science and Manufacturing*, vol. 147, Aug. 2021, p. 106454, <https://doi.org/10.1016/j.compositesa.2021.106454>.
- [6] Simacek, Pavel, et al. "Role of Resin Percolation in Gap Filling Mechanisms during the Thin Ply Thermosetting Automated Tape Placement Process." *Composites. Part A, Applied Science and Manufacturing*, vol. 152, 1 Jan. 2022, pp. 106677–106677, <https://doi.org/10.1016/j.compositesa.2021.106677>.